SIAM J. APPL. MATH.
Vol. 74, No. 3, pp. 885–897

STATIONARY WIGNER EQUATION WITH INFLOW BOUNDARY CONDITIONS: WILL A SYMMETRIC POTENTIAL YIELD A SYMMETRIC SOLUTION?*

RUO LI†, TIAO LU‡, AND ZHANGPENG SUN§

Abstract. Based on the well-posedness of the stationary Wigner equation with inflow boundary conditions given in [A. Arnold, H. Lange, and P.F. Zweifel, *J. Math. Phys.*, 41 (2000), pp. 7167–7180] we prove without any additional prerequisite conditions that the solution of the Wigner equation with inflow boundary conditions will be symmetric only if the potential is symmetric. This improves the result in [D. Taj, L. Genovese, and F. Rossi, *Europhys. Lett.*, 74 (2006), pp. 1060–1066], which depends on the convergence of the solution formulated in the Neumann series. By numerical studies, we present the convergence of the numerical solution to the symmetric profile for three different numerical schemes. This implies that the upwind schemes can also yield a symmetric numerical solution, contrary to the argument given in [D. Taj, L. Genovese, and F. Rossi, *Europhys. Lett.*, 74 (2006), pp. 1060–1066].

Key words. Wigner equation, inflow boundary conditions, well-posedness

AMS subject classifications. 81S30, 65N06, 65N12, 35B06

DOI. 10.1137/130941754

1. Introduction.

When device dimensions reduce to the nanometer scale, the quantum effects, such as size quantization and tunneling, become important in studying the properties of devices [15]. An appealing tool describing quantum transport is Wigner's formalism [11]. It is based on the Wigner distribution defined in the phase space as a Fourier transform of the density operator [16]. The governing equation of the Wigner distribution is the Wigner equation, which is very similar to its classical counterpart, the Boltzmann equation. As the Planck constant $\hbar$ goes to zero, the Wigner equation reduces to the Boltzmann equation under some conditions [10]. The strong analogy between Wigner and Boltzmann formalisms makes it possible to adapt the mature techniques used by the Boltzmann equation for the Wigner equation, e.g., inflow boundary conditions and Fermi's golden rule for scattering [4]. When the Coulomb interaction among particles is included, the self-consistent Wigner–Poisson equations could be considered; see, e.g., [9]. Since Frensley successfully reproduced the negative differential resistance by using an upwind finite difference method for the Wigner equation with inflow boundary conditions, numerical simulations based on the Wigner equation and the Wigner–Poisson equations for quantum devices such as resonant tunneling diodes have grown increasingly [5, 6, 3, 17, 13]. The inflow boundary conditions are of Dirichlet type in the Wigner phase space and specify the inflow on the left and right contacts. Typically, the distribution of the injected particles is taken as a Fermi–Dirac distribution [5]. We note that there are other types of boundary

*Received by the editors October 17, 2013; accepted for publication (in revised form) April 14, 2014; published electronically June 24, 2014. This work was supported in part by the National Basic Research Program of China (2011CB309704) and the NSFC (91230107, 11325102, 91330205).
http://www.siam.org/journals/siap/74-3/94175.html
†HEDPS & CAPT, LMAM & School of Mathematical Sciences, Peking University, Beijing 100871, China (rli@math.pku.edu.cn).
‡Corresponding author. HEDPS & CAPT, LMAM & School of Mathematical Sciences, Peking University, Beijing 100871, China (tlu@math.pku.edu.cn).
§School of Mathematical Sciences, Peking University, Beijing 100871, China (sunzhangpeng@pku.edu.cn).

conditions for the Wigner equation, e.g., absorbing boundary conditions [1] and device adaptive inflow boundary conditions [7]. The inflow boundary conditions break up the equivalence of the Wigner(–Poisson) formalism and the Schrödinger(–Poisson) formalism, and this makes the mathematical analysis very difficult for the Wigner equation and much more difficult for the nonlinear Wigner–Poisson equations [2]. So in this paper, we will focus on the linear case.

The stationary dimensionless Wigner equation can be written as [16]

$$v\frac{\partial f(x,v)}{\partial x} + \int \mathrm{d}v' V_w(x, v-v') f(x,v') = 0, \tag{1.1}$$

where the Wigner potential $V_w(x,v)$ is related to the potential $V(x)$ through

$$V_w(x,v) = \frac{\mathrm{i}}{2\pi}\int \mathrm{d}y\ \mathrm{e}^{-\mathrm{i}vy}\left[V(x+y/2) - V(x-y/2)\right]. \tag{1.2}$$

We are considering the inflow boundary conditions proposed in [5] and analyzed in [2, 14], which specify the inflow electron distribution function $f(-l/2, v)$, $v > 0$, at the left contact ($x = -l/2$) and $f(l/2, v)$, $v < 0$, at the right contact ($x = l/2$). In [14], the Wigner equation with a symmetric potential ($V(-x) = V(x)$) is considered. It was declared in [14] that (1.1) with a symmetric potential always gives a Wigner function symmetric in the spatial coordinate, $f(x,v) = f(-x,v)$, no matter what the profile of the injected carrier distribution is. Actually, it is not true for all the symmetric potential functions. For example, when $V(x) = 1 - x^2/2$, the Wigner equation will reduce to its classical counterpart, the Boltzmann equation (the Liouville equation):

$$v\frac{\partial f(x,v)}{\partial x} + x\frac{\partial f(x,v)}{\partial v} = 0. \tag{1.3}$$

One may figure out the solution of (1.3) by examining rolling balls to a hill with a shape $V(x) = 1 - x^2/2$. When one rolls a ball with the initial kinetic energy less than the height of $V(x)$ (which is 1 at $x = 0$), it is impossible to find the ball on the right-hand side. This implies that a symmetric potential cannot ensure a symmetric distribution, provided that the inflow boundary conditions are asymmetric. Let us put forward a question:

> *For which class of symmetric potentials does* (1.1) *always have a symmetric solution for any inflow boundary condition?*

In this paper, we answer this question partially by proving that for a symmetric and periodic potential with a period l, the Wigner equation (1.1) with inflow boundary conditions has one and only one symmetric solution. The proof hereafter is based on the elegant approach of the well-posedness of the stationary Wigner equation with inflow boundary conditions in [2]. The proof in [2] is given only for the discrete velocity version of the Wigner equation, provided that 0 is excluded from the discrete velocity points adopted. In this paper, we consider the continuous version of the Wigner equation (1.1) with the periodic condition of the potential function. By the periodicity of $V(x)$, we first simplify the Wigner equation to a form equivalent to its discrete velocity version. Then we are able to make use of the well-posedness theorem in [2] to prove the symmetric property.

In [14], a central finite difference method was proposed to provide a symmetric solution. It was declared therein that the numerical solution will give an asymmetric solution in the case of the first-order upwind finite difference scheme being used. This indicates that the first-order upwind finite difference scheme will not converge

to the exact solution at all, which is predicted theoretically to be symmetric in x. It was argued that the strange numerical behavior is due to the central scheme being more physical than the upwind scheme. Doubting this point of view, we revisit the numerical example in [14] using three different numerical schemes, including the two schemes used in [14] and a second-order upwind finite difference scheme. Our numerical results demonstrate that the first-order upwind finite difference method and the second-order upwind finite difference scheme can also give symmetric solutions as long as the grid size is small enough. Moreover, the symmetry of the numerical solution can be quantitatively bounded by the accuracy of the numerical solution. Thus we find out that whether or not the numerical solution is symmetric is related not only to the numerical scheme but also to the numerical accuracy.

The remainder of this paper is arranged as follows: In section 2, we prove the symmetry of the solution of (1.1) with a symmetric potential, and in section 3, the numerical study of the example in [14] is presented. A conclusion is drawn in section 4.

2. Symmetry of solution of (1.1) with symmetric potential. In general, the well-posedness of the boundary value problem (BVP) for the stationary Wigner equation

$$v\frac{\partial f(x,v)}{\partial x} + \int \mathrm{d}v' V_w(x, v-v') f(x,v') = 0, \quad x \in (-l/2, l/2),\ v \in \mathbb{R}, \tag{2.1}$$

with the inflow boundary conditions

$$f(-l/2, v) = f_b(v) \text{ for } v > 0; \quad f(l/2, v) = f_b(v) \text{ for } v < 0 \tag{2.2}$$

is an open problem [2].

At first, we expand the potential $V(x)$ into a Fourier series. The Fourier series is uniformly convergent to $V(x)$ under mild conditions, e.g., if $V(x)$ is periodic and continuous and its derivative $V'(x)$ is piecewise continuous. Particularly, if $V(x)$ is symmetric with respect to the y-axis, i.e., it is an even function, we can expand it into a cosine series. In this paper, we consider a special case in which the potential function $V(x)$ defining V_w through (1.2) is a periodic ($V(x+l) = V(x)$), even function with an absolutely convergent Fourier series, i.e.,

$$V(x) = a_0 + \sum_{n=1}^{\infty} a_n \cos(2n\kappa x), \tag{2.3}$$

where $\kappa = \frac{\pi}{l}$ and $\sum_{n=0}^{\infty} |a_n|$ is finite. Several sufficient conditions for $V(x)$ to have an absolutely convergent Fourier series are given in [8]; e.g., if $V(x)$ is absolutely continuous in $[-l/2, l/2]$ and $V'(x) \in L^2[-l/2, l/2]$, then $V(x)$ has an absolutely convergent Fourier series. We will prove that the BVP (2.1), (2.2) is well-posed, and its solution is symmetric, i.e., $f(x,v) = f(-x,v)$, $v \neq 0$, no matter what the profile of the injected carrier distribution is, provided that $V(x)$ has an expansion (2.3). For $V(x)$ with an expansion in (2.3), a direct calculation of (1.2) yields

$$V_w(x,v) = \sum_{n=1}^{\infty} a_n \sin(2n\kappa x) \left(\delta(v + n\kappa) - \delta(v - n\kappa)\right). \tag{2.4}$$

Thus, plugging (2.4) into the Wigner equation (2.1), we reformulate the stationary dimensionless Wigner equation as

$$v\frac{\partial f(x,v)}{\partial x}+\sum_{n=1}^{\infty}a_n\sin(2n\kappa x)\left(f(x,v+n\kappa)-f(x,v-n\kappa)\right)=0, \tag{2.5}$$

where $x\in(-l/2,l/2)$ and $v\in\mathbb{R}$.

Observing (2.5), one can see that v can be viewed as a parameter, (2.5) can be regarded as a set of ordinary differential equations, and $f(x,v)$ couples only with $f(v+n\kappa)$, $n\in\mathbb{Z}$. The BVP (2.5) with inflow boundary conditions (2.2) can be decoupled into independent ordinary differential systems indexed by $s\in(0,\kappa)$,

$$v_i^s\frac{\mathrm{d}f(x,v_i^s)}{\mathrm{d}x}+\sum_{n=1}^{\infty}a_n\sin(2n\kappa x)\left(f(x,v_{i+n}^s)-f(x,v_{i-n}^s)\right)=0,\quad x\in(-l/2,l/2),\ i\in\mathbb{Z}, \tag{2.6}$$

under the inflow boundary conditions

$$f(-l/2,v_i^s)=f_b(v_i)\text{ for }i\geqslant 0;\quad f(l/2,v_i^s)=f_b(v_i)\text{ for }i<0, \tag{2.7}$$

where $v_i^s=i\kappa+s$. Notice that we have to neglect the case $s=0$ from now on.

Remark 1. If $s=0$, (2.6) becomes an algebraic-differential system and its property is quite different, and it will bring difficulty to the theoretical analysis [2]. And to the authors' best knowledge, 0 is also excluded from the sampling velocity set in all numerical simulation papers; see, e.g., [5, 6].

Let $f_i^s(x)$ denote $f(x,v_i^s)$, and let the vector $\mathbf{f}^s(x)=(f_i^s(x),\ i\in\mathbb{Z})^T$ denote the discrete velocity Wigner function on the discrete velocity set $\mathbf{v}^s=\{v_i^s:=i\kappa+s,\ i\in\mathbb{Z}\}$. The discrete velocity $v_i^s\in\mathbb{R}$ is strictly increasing, i.e., $v_i^s<v_{i+1}^s$. Considering the singularity of the equation when $v=0$, we have excluded 0 from $\mathbf{v}^s$ by setting $s\neq 0$. Henceforth, we omit the superscript ^{s} of $f_i^s(x)$, $\mathbf{f}^s$, $\mathbf{v}^s$, and v_i^s when no confusion happens. Then we rewrite the stationary Wigner equation (2.6) to be its discrete counterpart as

$$\boldsymbol{T}\mathbf{f}_x-\boldsymbol{A}(x)\mathbf{f}=0,\quad -l/2<x<l/2, \tag{2.8}$$

subject to the inflow boundary conditions (2.7) rewritten as

$$f_i(-l/2)=f_b(v_i)\text{ for }i\geqslant 0;\quad f_i(l/2)=f_b(v_i)\text{ for }i<0, \tag{2.9}$$

with a given vector $\mathbf{f}_b=(f_b(v_i),\ i\in\mathbb{Z})^T$. Here, $\boldsymbol{T}$ is a diagonal matrix given as

$$\boldsymbol{T}=\mathrm{diag}\{\ldots,v_{-2},v_{-1},v_0,v_1,v_2,\ldots\}$$

and

$$\boldsymbol{A}(x)=\begin{pmatrix}
 & \ddots & & & & & \\
\cdots & a_1\sin(2\kappa x) & 0 & -a_1\sin(2\kappa x) & -a_2\sin(4\kappa x) & -a_3\sin(6\kappa x) & \cdots\\
\cdots & a_2\sin(4\kappa x) & a_1\sin(2\kappa x) & 0 & -a_1\sin(2\kappa x) & -a_2\sin(4\kappa x) & \cdots\\
\cdots & a_3\sin(6\kappa x) & a_2\sin(2\kappa x) & a_1\sin(2\kappa x) & 0 & -a_1\sin(2\kappa x) & \cdots\\
 & & & & & \ddots &
\end{pmatrix},$$

which is a skew-symmetric matrix.

Let $l^2(\mathbb{Z}; w_i)$ denote the linear space of vectors, $\mathbf{f}(x) = (f_i^s(x),\ i \in \mathbb{Z})^T$, equipped with the canonical weighted l^2-norm

$$\|\mathbf{f}\|_{2,w} = \left(\sum_{i\in\mathbb{Z}} w_i |f_i|^2\right)^{1/2},$$

where $w_i = |w(v_i)|$ and $w(v)$ is a weight function. Particularly, when $w(v) = v$, we denote $l^2(\mathbb{Z}; w_i)$ by H_v with the norm

$$\|\mathbf{f}\|_{H_v} \equiv \|\mathbf{f}\|_{2,v} = \left(\sum_{i\in\mathbb{Z}} |v_i||f_i|^2\right)^{1/2},$$

and when $w(v) = 1$, we denote $l_2(\mathbb{Z}, w_i)$ by H with the norm

$$\|\mathbf{f}\|_H \equiv \|\mathbf{f}\|_{2,1} = \left(\sum_{i\in\mathbb{Z}} |f_i|^2\right)^{1/2}.$$

Since H is the usual (nonweighted) l^2 space, we denote $\|\cdot\|_{2,1}$ by $\|\cdot\|_2$. H is a real Hilbert space with the natural inner product $\langle \mathbf{f}, \mathbf{g}\rangle = \sum_{i\in\mathbb{Z}} f_i g_i$. Let $B(H)$ denote the space of all bounded linear operators on H. Then we have the following lemma.

LEMMA 1. *If the Fourier coefficients of $V(x)$, $\{a_n\}_{n=0}^{\infty} \in l^1$, then $\boldsymbol{A}(x) \in B(H)$.*

Proof. Observing

$$(\boldsymbol{A}(x)\mathbf{f}(x))_k = \sum_{i=-\infty}^{\infty} a_{|k-i|} \sin(2(k-i)\kappa x) f_i(x),$$

one can find that $\boldsymbol{A}(x)\mathbf{f}(x)$ is a discrete convolution, i.e.,

$$\boldsymbol{A}(x)\mathbf{f}(x) = \mathbf{V}_d(x) * \mathbf{f}(x),$$

where $\mathbf{V}_d(x) = \{a_{|i|} \sin(2i\kappa x),\ i \in \mathbb{Z}\}$. We can apply Young's inequality to the discrete convolution

$$\boldsymbol{A}(x)\mathbf{f}(x) = \mathbf{V}_d(x) * \mathbf{f}(x)$$

to have

$$\|\boldsymbol{A}(x)\mathbf{f}(x)\|_2 = \|\mathbf{V}_d(x) * \mathbf{f}(x)\|_2 \leqslant \|\mathbf{V}_d(x)\|_1 \|\mathbf{f}(x)\|_2.$$

On the other hand, we have

$$\|\mathbf{V}_d\|_1 = \sum_{i=-\infty}^{\infty} |a_{|i|} \sin(2i\kappa x)| \leqslant 2\sum_{n=1}^{\infty} |a_n| \leqslant 2\|\{a_n\}_{n=0}^{\infty}\|_1 < \infty.$$

Thus by noting that the H-norm is the same as the l^2-norm, we have

$$\|\boldsymbol{A}(x)\mathbf{f}(x)\|_H \leqslant 2\|\{a_n\}_0^{\infty}\|_1 \|\mathbf{f}\|_H,$$

which gives the conclusion that $\boldsymbol{A}(x) \in B(H)$ and $\|\boldsymbol{A}(x)\| \leq 2\|\{a_n\}_0^{\infty}\|_1$. ∎

The proof of the well-posedness of the discrete velocity problem has been given in [2], and here we present the conclusion below.

LEMMA 2 (see [2, Theorem 3.3]). *Assume $\mathbf{f}_b = (f_b(v_i),\ i \in \mathbb{Z})^T \in H_v$, and let $\boldsymbol{A}(x) \in B(H)$ be skew-symmetric for all $x \in [-l/2, l/2]$. Then one has the following:*

(a) *If* $\boldsymbol{A} \in L^1((-l/2, l/2), B(H))$*, the BVP* (2.8), (2.9) *has a unique mild solution* $\mathbf{f}(x) \in W^{1,1}((-l/2, l/2), H_v)$*. Also,* $\boldsymbol{T}\mathbf{f}_x \in L^1((-l/2, l/2), H)$*.*

(b) *If* $\boldsymbol{A}(x)$ *is strongly continuous in* x *on* $[-l/2, l/2]$ *and uniformly bounded in the norm of* $B(H)$ *on* $[-l/2, l/2]$*, then the solution from* (a) *is classical, i.e.,* $\mathbf{f} \in C^1([-l/2, l/2], H_v)$*. Also,* $\boldsymbol{T}\mathbf{f}_x \in C([-l/2, l/2], H)$*.*

Now we are ready for the following theorem.

THEOREM 1. *Assume* $V(x)$ *is a periodic, even function with an absolutely convergent Fourier series, i.e.,* $\{a_n\}_{n=0}^{\infty} \in l^1$*. For all* $s \in (0, \kappa)$*, let* $\mathbf{f}_b = (f_b(v_i),\, i \in \mathbb{Z})^T \in H_v$ *be defined by* (2.9) *on* $\mathbf{v}^s$*. Then the BVP* (2.8), (2.9) *has a unique solution* $\mathbf{f}(x)$*, and for the discrete velocity Wigner function on the discrete velocity set* $\mathbf{v}^s$*,* $\mathbf{f}(x)$ *is a mild solution in* $W^{1,1}((-l/2, l/2), H_v)$*.*

Proof. It is clear that for all $s \in (0, \kappa)$, the corresponding discrete velocity Wigner function $\mathbf{f}(x)$ satisfies the BVP (2.8), (2.9). By Lemma 1, $\boldsymbol{A}(x) \in B(H)$, and by the assumption, $\mathbf{f}_b = (f_b(v_i),\, i \in \mathbb{Z})^T \in H_v$, and thus the requirement of Lemma 2 is fulfilled. Applying Lemma 2, we have that $\mathbf{f}(x) \in W^{1,1}((-l/2, l/2), H_v)$. This ends the proof. ∎

Based on the well-posedness of the above Wigner equation, the solution of the BVP (2.8), (2.9) satisfies the following initial value problem (IVP):

$$\frac{\mathrm{d}\mathbf{f}(x)}{\mathrm{d}x} = \boldsymbol{T}^{-1}\boldsymbol{A}(x)\mathbf{f}(x), \quad x \in (-l/2, l/2), \tag{2.10}$$

with $\mathbf{f}(x)$ at $x = x_1$ being a given vector. One can define a propagator $\mathcal{T}_{[x_1,x_2]}$ via the solution of the IVP (2.10) [12], i.e.,

$$\mathbf{f}(x_2) = \mathcal{T}_{[x_1,x_2]}\mathbf{f}(x_1).$$

Clearly, the operator $\mathcal{T}_{[x_1,x_2]}$ is invertible and

$$\mathcal{T}^{-1}_{[x_1,x_2]} = \mathcal{T}_{[x_2,x_1]}.$$

More properties of $\mathcal{T}_{[x_1,x_2]}$ can be found in [12].

Moreover, if the potential is symmetric, i.e., $V(x) = V(-x)$, we have the following lemma.

LEMMA 3. *If* $V(x)$ *is a periodic, even function with an absolutely convergent Fourier series, i.e.,* $\{a_n\}_{n=0}^{\infty} \in l^1$*, then* $\mathcal{T}_{[0,x]} = \mathcal{T}_{[0,-x]}$ *for all* $x \in (-l/2, l/2)$*.*

Proof. The IVP (2.10) can be recast into an integral equation

$$\mathbf{f}(x) = \mathbf{f}(x_1) + \int_{x_1}^{x} \boldsymbol{T}^{-1}\boldsymbol{A}(y)\mathbf{f}(y)\,\mathrm{d}y = \mathbf{f}(x_1) + K_{[x_1,x_2]}\mathbf{f}(x), \quad x \in [x_1, x_2] \text{ or } x \in [x_2, x_1], \tag{2.11}$$

where $K_{[x_1,x_2]}$ is defined by

$$K_{[x_1,x_2]}\mathbf{f}(x) = \int_{x_1}^{x} \boldsymbol{T}^{-1}\boldsymbol{A}(y)\mathbf{f}(y)\,\mathrm{d}y \quad \text{for } x \in [x_1, x_2] \text{ or } x \in [x_2, x_1].$$

We have that

$$\|K_{[x_1,x_2]}\mathbf{f}(x)\|_{H,\infty} \leqslant \frac{C|x_1 - x_2|}{\min_{i\in\mathbb{Z}} |v_i|}\|\mathbf{f}(x)\|_{H,\infty},$$

where the norm of a vector function $\mathbf{g}(x)$, $x \in [x_1, x_2]$, is defined by

$$\|\mathbf{g}(x)\|_{H,\infty} = \sup_{x\in[x_1,x_2]}\|\mathbf{g}(x)\|_H,$$

and C is twice the l^1-norm of the Fourier coefficients of $V(x)$. Noticing that $\min_{j\in\mathbb{Z}}|v_j| > 0$, we have that

$$\|K_{[x_1,x_2]}\|_{C([x_1,x_2],H)} < 1$$

if $|x_1 - x_2| < \tilde{\delta} = \min_{j\in\mathbb{Z}}|v_j|/C > 0$. By applying the Neumann series to (2.11), we have that

$$\mathbf{f}(x) = (I - K_{[x_1,x_2]})^{-1}\mathbf{f}^{(0)}(x) = \sum_{n=0}^{\infty} K^n_{[x_1,x_2]}\mathbf{f}^{(0)}(x),$$

or

$$\mathbf{f}(x) = \lim_{n\to\infty} \mathbf{f}^{(n)}(x), \tag{2.12}$$

where

$$\begin{aligned} &\mathbf{f}^{(0)}(x) = \mathbf{f}(x_1), \quad x \in [x_1, x_2] \text{ or } [x_2, x_1], \\ &\mathbf{f}^{(n+1)}(x) = \mathbf{f}(x_1) + K_{[x_1,x_2]}\mathbf{f}^{(n)}(x), \quad x \in [x_1, x_2] \text{ or } [x_2, x_1],\ n = 0, 1, \ldots. \end{aligned} \tag{2.13}$$

Obviously, the Neumann series is convergent if $|x_2 - x_1| \le \delta < \tilde{\delta}$. $V(x)$ is symmetric, i.e., $V(x) = V(-x)$, so we see that $\boldsymbol{A}(-x) = -\boldsymbol{A}(x)$. At the same time, $\mathbf{f}^{(0)}(x)$, $x \in [-\delta, \delta]$, is symmetric (actually, $\mathbf{f}^{(0)}(x) = \mathbf{f}(0)$, $x \in [-\delta, \delta]$, is a constant vector function of x), so we have

$$\begin{aligned} K_{[0,-\delta]}\mathbf{f}^{(0)}(x) &= \int_0^{-x} \boldsymbol{T}^{-1}\boldsymbol{A}(y)\mathbf{f}^{(0)}(y)\,\mathrm{d}y \\ &= \int_0^{x} \boldsymbol{T}^{-1}\boldsymbol{A}(-y)\mathbf{f}^{(0)}(-y)\,\mathrm{d}(-y) \\ &= \int_0^{x} \boldsymbol{T}^{-1}(-\boldsymbol{A}(y))\mathbf{f}^{(0)}(y)(-\,\mathrm{d}y) \\ &= \int_0^{x} \boldsymbol{T}^{-1}\boldsymbol{A}(y)\mathbf{f}^{(0)}(y)\,\mathrm{d}y = K_{[0,\delta]}\mathbf{f}^{(0)}(x), \end{aligned}$$

which implies $\mathbf{f}^{(1)}(-x) = \mathbf{f}^{(1)}(x)$. It is easy to see that we can obtain $\mathbf{f}^{(n)}(-x) = \mathbf{f}^{(n)}(x)$, $n = 2, 3, \ldots$, and thus we have $\mathbf{f}(x) = \mathbf{f}(-x)$, $x \in [-\delta, \delta]$, i.e.,

$$\begin{aligned} \mathcal{T}_{[0,-x]}\mathbf{f}(0) &= \mathbf{f}(-x) = \sum_{n=0}^{\infty} K[0,-\delta]^n\mathbf{f}^{(0)}(x) \\ &= \sum_{n=0}^{\infty} K[0,\delta]^n\mathbf{f}^{(0)}(x) = \mathbf{f}(x) = \mathcal{T}_{[0,x]}\mathbf{f}(0), \quad x \in [0,\delta]. \end{aligned}$$

Thus $\mathcal{T}_{[0,x]} = \mathcal{T}_{[0,-x]}$ for $|x| \leqslant \delta$. We have shown that $\mathbf{f}(-x) = \mathbf{f}(x)$ for $x \in [-\delta, \delta]$. Furthermore, we define $\mathbf{f}^0(x) = \mathbf{f}(-\delta)$, $x \in [-\delta, -2\delta]$, $\mathbf{f}^{(0)}(x) = \mathbf{f}(\delta)$, $x \in [\delta, 2\delta]$, and it is easy to see that $\mathbf{f}^{(0)}(-x) = \mathbf{f}^{(0)}(x), x \in [-\delta, -2\delta] \cup [\delta, 2\delta]$. Then using the same

argument, we have for $x \in [-\delta, -2\delta]$,

$$\begin{aligned} K_{[-\delta,-2\delta]}\mathbf{f}^{(0)}(x) &= \int_{-\delta}^{x} T^{-1}\boldsymbol{A}(y)\mathbf{f}^{0}(y)\,\mathrm{d}y \\ &= \int_{\delta}^{-x} T^{-1}\boldsymbol{A}(-y)\mathbf{f}^{0}(-y)\,\mathrm{d}(-y) \\ &= \int_{\delta}^{-x} T^{-1}(-\boldsymbol{A}(y))\mathbf{f}^{(0)}(y)(-\,\mathrm{d}y) \\ &= \int_{\delta}^{-x} T^{-1}\boldsymbol{A}(y)\mathbf{f}^{(0)}(y)\,\mathrm{d}y = K_{[\delta,2\delta]}\mathbf{f}^{(0)}(-x), \end{aligned}$$

and $K_{[-\delta,-2\delta]}\mathbf{f}^{(n)}(x) = K_{[\delta,2\delta]}\mathbf{f}^{(n)}(-x)$, $n = 1, 2, \ldots$, and thus

$$\mathbf{f}(x) = \mathcal{T}_{[0,x]}\mathbf{f}(0) = \mathcal{T}_{[0,-x]}\mathbf{f}(0) = \mathbf{f}(-x) \quad \forall x \in [-2\delta, -\delta] \cup [\delta, 2\delta].$$

This implies that the domain valid for $\mathcal{T}_{[0,x]} = \mathcal{T}_{[0,-x]}$ can be continuously extended. Thus we conclude that $\mathcal{T}_{[0,x]} = \mathcal{T}_{[0,-x]}$ for all $x \in (-l/2, l/2)$. ∎

By the lemma above, we arrive at the following theorem.

THEOREM 2. *If $V(x)$ is a periodic, even function with an absolutely convergent Fourier series, the solution of the BVP* (2.1), (2.2) *satisfies*

$$f(x, v) = f(-x, v) \quad \forall v \in \mathbb{R},\ v \neq n\kappa,\ n \in \mathbb{Z},$$

for any inflow boundary condition.

Proof. Since $v \neq n\kappa$, $n \in \mathbb{Z}$, there exists $s \in (0, \kappa)$ such that $v \in \mathbf{v}^s$. Thus $f(x, v)$ is an entry of $\mathbf{f}(x)$, which is the Wigner function value at the discrete velocity set $\mathbf{v}^s$. From Lemma 3, we have that the discrete velocity Wigner function on $\mathbf{v}^s$ satisfies

$$\mathbf{f}(x) = \mathcal{T}_{[0,x]}\mathbf{f}(0) = \mathcal{T}_{[0,-x]}\mathbf{f}(0) = \mathbf{f}(-x).$$

Then we have $f(x, v) = f(-x, v)$. ∎

Remark 2. When $v = 0$, the problem may be reduced to an ordinary differential equation system in the same form as (2.8) and (2.9). The equation at $s = 0$ in (2.6) is formally turned into an algebraic constraint as

$$\sum_{n=1}^{\infty} a_n \sin(2n\kappa x)\,(f_n(x) - f_{-n}(x)) = 0.$$

It is clear that if $f(x, 0) \equiv 0$, the well-posedness of the system is still valid. If $f(x, 0) \not\equiv 0$, this algebraic constraint above cannot always be fulfilled, and thus the existence of the solution is negative. On the other hand, the term involving the derivative in x at $v = 0$ may be a $0 \times \infty$ form since the derivative $\partial f(x, 0)/\partial x$ is not bounded by any regularity. This makes the algebraic constraint obtained above by formally dropping the first term doubtable, which requires further investigation.

3. Numerical study on symmetry of solution. In order to verify the theoretical analysis in Theorem 2, we revisit the example in [14] which considers a particular potential profile $V(x) = V_0(1 + \cos(2\kappa x))$. The corresponding Wigner potential V_w in (2.4) is given simply by

$$V_w(x, v) = V_0 \sin(2\kappa x)\,(\delta(v + \kappa) - \delta(v - \kappa))\,. \tag{3.1}$$

The boundary conditions are extremely simple, too. A monoenergetic carrier injects only from the left boundary; i.e., we set $f_b(v_i)$ in (2.9) to be

$$f_b(v_i) = \begin{cases} 1 & \text{if } i = 0, \\ 0 & \text{else,} \end{cases} \tag{3.2}$$

where $v_i = (i + 1/2)\kappa$, which means $s = \kappa/2$ (the index of the differential system (2.6)).

In this section, we will solve the ordinary differential system (2.8)–(2.9) with V_w in (3.1), which reduces to

$$v_i \frac{\mathrm{d}f_i(x)}{\mathrm{d}x} = V_0 \sin(2\kappa x)\left(f_{i+1}(x) - f_{i-1}(x)\right), \quad x \in (-l/2, l/2),\ i \in \mathbb{Z}, \tag{3.3}$$

under inflow boundary conditions (2.9) with inflow data given in (3.2).

The other parameters are set as $V_0 = 20$ and $l = 1$, which gives $\kappa = \pi/l = \pi$. The kinetic energy is $v_0^2/2$, which is lower than the height of the potential energy in the middle of the device. If using the classic mechanics (the Liouville equation or the Boltzmann equation), one cannot see the carrier in the right part of the device. This implies that the classic mechanics will yield an asymmetric solution.

In the following part of the section, we will show that the numerical solution of the Wigner equation will be symmetric using three numerical schemes. The first scheme is the first-order upwind finite difference method [5], and the other two are second-order finite difference methods. The second scheme is the second-order upwind finite difference method used in many numerical simulation papers; see, e.g., [6]. The authors of [14] used the first-order upwind finite difference method and failed to get a symmetric solution, so they proposed a central finite difference method based on a physical argument, which is adopted as our third scheme.

3.1. Three finite difference schemes. We implement the finite difference methods on a uniform mesh. The x-domain $[-l/2, l/2]$ is discretized with $N_x + 1$ equally distanced grid points $x_j = j\Delta x$, $j = 0, 1, \ldots, N_x$, where $\Delta x = l/N_x$. We have to truncate $i \in \mathbb{Z}$ into a finite set $\{i : M \leqslant i < M\}$. M depends on the inflow data and the potential strength V_0, and in our current example, we set $M = 40$, which is found large enough for our numerical example. We denote $f_i(x)$ at $x = x_j$ by $f_{i,j}$. The first-order upwind finite difference scheme is obtained by approximating $\frac{\mathrm{d}f_i(x)}{\mathrm{d}x}\big|_{x_j}$ with

$$\left.\frac{\mathrm{d}f_i(x)}{\mathrm{d}x}\right|_{x_j} \approx \begin{cases} \frac{f_{i,j+1} - f_{i,j}}{\Delta x} & \text{if } v_i < 0, \\ \frac{f_{i,j} - f_{i,j-1}}{\Delta x} & \text{if } v_i > 0, \end{cases}$$

thus yielding the finite difference equation of (3.3) as

$$\begin{cases} v_i \dfrac{f_{i,j+1} - f_{i,j}}{\Delta x} = g_{i,j}, & v_i < 0,\ j = 0, 1, \ldots, N_x - 1, \\ v_i \dfrac{f_{i,j} - f_{i,j-1}}{\Delta x} = g_{i,j}, & v_i > 0,\ j = 1, 2, \ldots, N_x, \end{cases} \tag{3.4}$$

where

$$g_{i,j} = V_0 \sin(2\kappa x_j)(f_{i-1,j} - f_{i+1,j}). \tag{3.5}$$

The second-order upwind finite difference method is obtained by approximating $\frac{\mathrm{d}f_i(x)}{\mathrm{d}x}\big|_{x_j}$ with

$$\frac{\mathrm{d}f_i(x)}{\mathrm{d}x}\bigg|_{x_j} \approx \begin{cases} \dfrac{-f_{i,j+2}+4f_{i,j+1}-3f_{i,j}}{2\Delta x}, & v_i<0, \\ \dfrac{f_{i,,j-2}-4f_{i,j-1}+3f_{i,j}}{2\Delta x}, & v_i>0. \end{cases} \tag{3.6}$$

The second-order upwind scheme includes three nodes, so the first-order upwind scheme is used in the boundary cell instead of the second-order one.

Both upwind schemes approximate $\frac{\mathrm{d}f_i}{\mathrm{d}x}$ at the grid point x_j using the grid points only on one side, while the central difference method proposed in [14] approximates $\frac{\mathrm{d}f_i(x)}{\mathrm{d}x}$ at $x_{j+1/2}=(x_j+x_{j+1})/2$ using the grid points x_j and x_{j+1}. That is, the central scheme approximates $\frac{\mathrm{d}f_i(x)}{\mathrm{d}x}\big|_{x_{j+1/2}}$ with

$$\frac{\mathrm{d}f_i(x)}{\mathrm{d}x}\bigg|_{x_{j+1/2}} \approx \frac{f_{i,j+1}-f_{i,j}}{\Delta x}. \tag{3.7}$$

Then the right-hand side of (3.3) at $x_{j+1/2}$ is approximated by the average of its values at x_j and x_{j+1}. Finally, the central scheme results in a difference equation as follows:

$$\begin{cases} v_i\dfrac{f_{i,j+1}-f_{i,j}}{\Delta x}=\dfrac{g_{i,j+1}+g_{i,j}}{2}, & v_i<0,\ j=0,1,\dots,N_x-1, \\ v_i\dfrac{f_{i,j}-f_{i,j-1}}{\Delta x}=\dfrac{g_{i,j+1}+g_{i,j}}{2}, & v_i>0,\ j=1,2,\dots,N_x, \end{cases} \tag{3.8}$$

where $g_{i,j}$ is given in (3.5).

3.2. Numerical results. We solve (3.3) using the first-order upwind finite difference method on different meshes with grid numbers $N_x=100,200,400,800,1600$. The numerical results show us that the Wigner distribution and the density function are clearly not symmetric in the spatial coordinate. This may be the reason why the authors of [14] declare that the symmetric solution cannot be obtained by the upwind scheme. But we keep refining the mesh by using $N_x=3200,\dots,25600$; the numerical results tend to be symmetric, as expected, which means that the first-order upwind scheme can also give us a symmetric numerical solution.

We solve (3.3) using the two second-order methods on the mesh with the grid number $N_x=100$. The Wigner distribution obtained by using the central finite difference method with $N_x=100$ is shown in Figure 1. We can see from the figure that

1. the Wigner distribution function is strongly symmetric with respect to x;
2. the incident particles with low energy can tunnel through the barrier;
3. the Wigner potential plays the role of a scattering mechanism and scatters carriers to higher energy states; and
4. the Wigner distribution function is negative in some regions, which is distinct from the classic distribution function.

By using the three schemes, we compute the density $n(x_j)$ defined by

$$n(x_j)=\sum_{i=-\infty}^{+\infty} f_i(x_j). \tag{3.9}$$

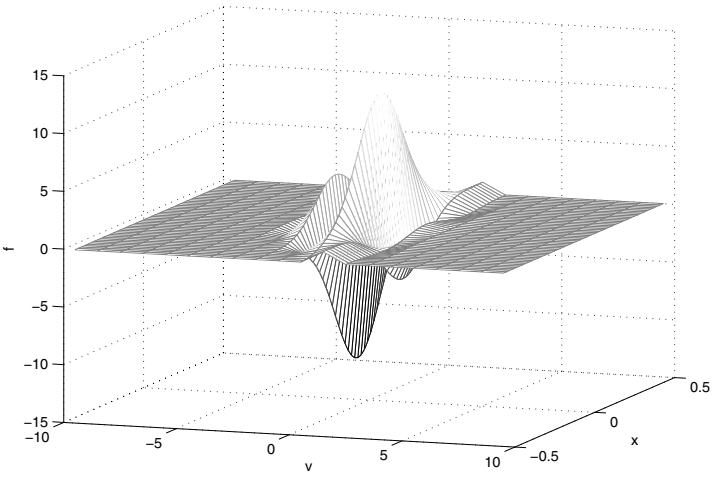

FIG. 1. *The distribution function obtained by using the central scheme on the mesh with* $N_x = 100$.

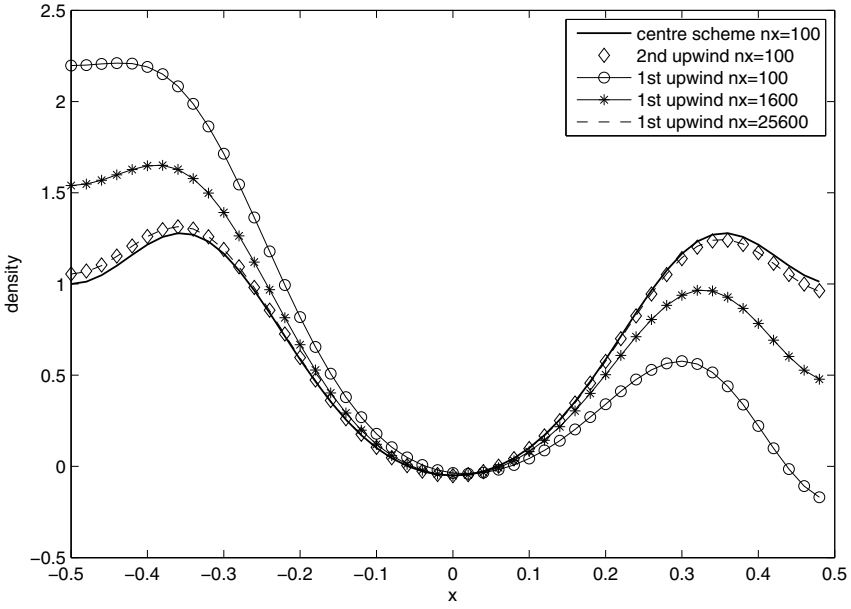

FIG. 2. *Density calculated by using the three schemes.*

The numerical densities obtained by using three schemes are shown in Figure 2, and the symmetric property can be observed both for the first-order method on the mesh with $N_x = 25600$ and for the second-order methods on the mesh with $N_x = 100$. Also, it can seen from Figure 2 that the numerical density obtained by using the

TABLE 1

Symmetry errors of the three schemes: the first-order upwind finite difference method (UFD1), the second-order upwind finite difference method (UFD2), and the central finite difference method (CFD).

Scheme \ N_x	100	400	1600	6400	25600
UFD1	1.03	0.7666	0.4185	0.1502	0.0422
UFD2	0.0462	7.446e-4	1.151e-5		
CFD	2.5966e-16				

second-order upwind scheme with $N_x = 100$ is almost coincident with that obtained by the first-order upwind scheme with $N_x = 25600$, and that the central scheme yields a perfectly symmetric density.

Figure 2 gives us an intuitive understanding of the symmetry of the solution. Next, to quantitatively compare the three schemes we define a symmetry error as

$$e_{\text{sym}} = \int \mathrm{d}v \int \mathrm{d}x |f(x,v) - f(-x,v)|. \tag{3.10}$$

Numerically, the symmetry error can be approximated by

$$\tilde{e}_{\text{sym}} = \sum_i \sum_j |f_i(x_j) - f_i(-x_j)| \Delta x. \tag{3.11}$$

The numerical symmetry errors obtained by using different schemes are collected in Table 1. As shown in Table 1, the numerical solution obtained by using the first-order upwind scheme becomes more and more symmetric as the mesh is refined, the symmetry error of the second-order upwind scheme with $N_x = 100$ is about the same as the first-order upwind scheme with $N_x = 25600$, and the solution obtained by the central scheme is perfectly symmetric due to the symmetry of the scheme itself. These are consistent with the results in Figure 2.

4. Conclusion. For the problem of whether the solution of the stationary Wigner equation with inflow boundary conditions will be symmetric if the potential is symmetric in [14], we gave a rigorous proof based on [2] under a mild assumption on the regularity of the potential. We concluded that a certain kind of continuous Wigner equation with inflow boundary conditions can be reduced to the discrete velocity case and thus is well-posed. Furthermore, we numerically studied the example in [14] and pointed out that the numerical solution will converge to the exact solution with symmetry, even when the numerical scheme adopted is not symmetric if only accuracy is enough.

REFERENCES

[1] A. ARNOLD, *On absorbing boundary conditions for quantum transport equations*, RAIRO Modél. Math. Anal. Numér., 28 (1994), pp. 853–872.

[2] A. ARNOLD, H. LANGE, AND P.F. ZWEIFEL, *A discrete-velocity, stationary Wigner equation*, J. Math. Phys., 41 (2000), pp. 7167–7180.

[3] A. ARNOLD AND C. RINGHOFER, *An operator splitting method for the Wigner–Poisson problem*, SIAM J. Numer. Anal., 33 (1996), pp. 1622–1643.

[4] D.K. FERRY AND S.M. GOODNICK, *Transport in Nanostructures*, Cambridge University Press, Cambridge, UK, 1997.

[5] W.R. FRENSLEY, *Wigner function model of a resonant-tunneling semiconductor device*, Phys. Rev. B, 36 (1987), pp. 1570–1580.

[6] K.L. Jensen and F.A. Buot, *Numerical aspects on the simulation of I-V characteristics and switching times of resonant tunneling diodes*, J. Appl. Phys., 67 (1990), pp. 2153–2155.
[7] H. Jiang, T. Lu, and W. Cai, *A device adaptive inflow boundary condition for Wigner equations of quantum transport*, J. Comput. Phys., 248 (2014), pp. 773–786.
[8] Y. Katznelson, *An Introduction to Harmonic Analysis*, 2nd ed., Dover, New York, 1976.
[9] N. Kluksdahl, A.M. Kriman, D.K. Ferry, and C. Ringhofer, *Self-consistent study of the resonant tunneling diode*, Phys. Rev. B., 39 (1989), pp. 7720–7735.
[10] P.-L. Lions and T. Paul, *Sur les mesure de Wigner*, Rev. Mat. Iberoamericana, 9 (1993), pp. 553–618.
[11] P.A. Markowich, C.A. Ringhofer, and C. Schmeiser, *Semiconductor Equations*, Springer, New York, 1990.
[12] A. Pazy, *Semigroups of Linear Operators and Applications to Partial Differential Equations*, 2nd ed., Springer, New York, 1992.
[13] S. Shao, T. Lu, and W. Cai, *Adaptive conservative cell average spectral element methods for transient Wigner equation in quantum transport*, Commun. Comput. Phys., 9 (2011), pp. 711–739.
[14] D. Taj, L. Genovese, and F. Rossi, *Quantum-transport simulations with the Wigner-function formalism: Failure of conventional boundary-condition schemes*, Europhys. Lett., 74 (2006), pp. 1060–1066.
[15] D. Vasileska, S.M. Goodnick, and G. Klimeck, *Computational Electronics: Semiclassical and Quantum Device Modeling and Simulation*, CRC Press, Taylor & Francis Group, New York, 2010.
[16] E. Wigner, *On the quantum correction for thermodynamic equilibrium*, Phys. Rev., 40 (1932), pp. 749–759.
[17] P.J. Zhao, D.L. Woolard, and H.L. Cui, *Multisubband theory for the origination of intrinsic oscillations within double-barrier quantum well systems*, Phys. Rev. B, 67 (2003), 085312.